Electromagnetics

A Technological Approach for Miniaturization of Three-Dimensional Inductive Levitation Microsuspensions

Emil R. Mamleyev[1], Achim Voigt[1], Ali Moazenzadeh[2], Jan G. Korvink[1]*, Manfred Kohl[1], and Kirill Poletkin[1,3]

[1] *Institute of Microstructure Technology, Karlsruhe Institute of Technology, 76344 Eggenstein-Leopoldshafen, Germany*
[2] *Voxalytic GmbH, 76228 Karlsruhe, Germany*
[3] *Innopolis University, 420500 Innopolis, Russia*
* *Member, IEEE*

Received 4 Apr 2022, revised 20 Apr 2022, accepted 4 May 2022, published 11 May 2022, current version 20 Jun 2022.

Abstract—In this letter, we report on a technological approach for miniaturization of a inductive levitating microsuspension based on nested three-dimensional (3-D) microcoil structures. In the developed approach, each 3-D microcoil is fabricated separately, beginning with the innermost and thus the smallest coil diameter of the nested microstructure. This helps to overcome fabrication restrictions due to the wire-bonding process and is primarily caused by the size of the bond-head and provides the opportunity to fabricate smaller nested 3-D microcoil structures. We fabricated a nested two-microcoil structure, the inner coil having a diameter of 1000 μm and 14 windings, the outer coil with a diameter of 1900 μm and eight windings, and demonstrated its application as an inductive levitating microsuspension. In particular, a fabricated 3-D inductive levitating microsuspension was able to levitate a 1100 μm diameter disc-shaped proof mass at a height up to 45 μm.

Index Terms—Electromagnetics, contactless suspension, microcoils, microfabrication.

I. INTRODUCTION

Levitation microsystems employ the phenomenon of electromagnetic levitation, eliminating a mechanical attachment between moving parts of a microsystem and offering the fundamental solution to overcome the domination of friction over inertial forces at the microscale. This fact has given birth to a new generation of microsensors and actuators with higher performance and wider operational capabilities [Poletkin 2020].

Electromagnetic levitation in microsystem devices is implemented by means of the concept of a contactless suspension (**CS**), which can be actualized, in particular, by employing a magnetic force field. The source of the magnetic force field can be static and time-variable magnetic fields. Hence, the CS using either static or time-variable magnetic fields can be classified as magnetic or inductive CS, respectively [Poletkin 2018].

Magnetic CS needs either a diamagnetic or a superconductive proof mass (**PM**). However, the strongest diamagnetic materials, pyrolitic carbon and bismuth [Simon 2001], are not traditional materials for microelectromechanical systems processing. For superconductive levitation, a cryogen environment must be maintained.

Magnetic levitation based on electromagnetic induction or inductive levitation does not suffer from the disadvantages mentioned above. However, the inductive CSs suffer from relatively high energy consumption. For instance, the prototype of inductive levitation microsuspension (**ILMS**) based on the two-coil design with the following diameters of 240 and 345 μm for levitation and stabilization coils, respectively, which was fabricated using planar technology, demonstrated the successful levitation of the PM of a 250 μm diameter at the height of ∼30 μm with the coil current of ∼1 A and the operating temperature around 600 °C as reported in Shearwood [2000]. Employing 3-D microcoils, which have been realized using 3-D wire-bonding technology by means of an automatic machine [Kratt 2010], the prototype of the 3-D ILMS (**3D-ILMS**) with diameters of 2000 and 3800 μm for levitation and stabilization coils, respectively, was fabricated by our group as reported in Lu [2014a, 2014b]. This fabricated prototype of 3D-ILMS having 20 and 12 number of windings for the levitation and stabilization coil, respectively, was able to successfully levitate a PM with the minimal diameter of 2800 μm and to reduce the operating temperature up to 120 °C. Using the same design of the nested microstructure but with integrating a magnetic core based on the polymer magnetic composite, our group showed the 3D-ILMS with the lowest operating temperature around 60 °C among all previously reported inductive CSs [Poletkin 2016].

Clearly, the further improvement in the energy performance of 3D-ILMS requires a nested coil structure of a smaller diameter. However, the fabrication process of a reduced size 3D-ILMS is restricted by a number of technological constraints, particularly the small gap between levitation and stabilization coil limiting access for the wire-bonder head.

In this letter, to overcome the mentioned above restrictions, we developed the technological approach in which each 3-D microcoil is fabricated separately, beginning with the smallest coil in diameter of the nested coil structure. The novel fabrication approach was employed to fabricate the nested two-microcoil structures having the inner coil with a diameter of 1000 μm and an outer one 1900 μm with 14 and eight number of windings, respectively, and to demonstrate its successful

Corresponding author: Kirill Poletkin (e-mail: k.poletkin@gmail.com).
Digital Object Identifier 10.1109/LMAG.2022.3174522

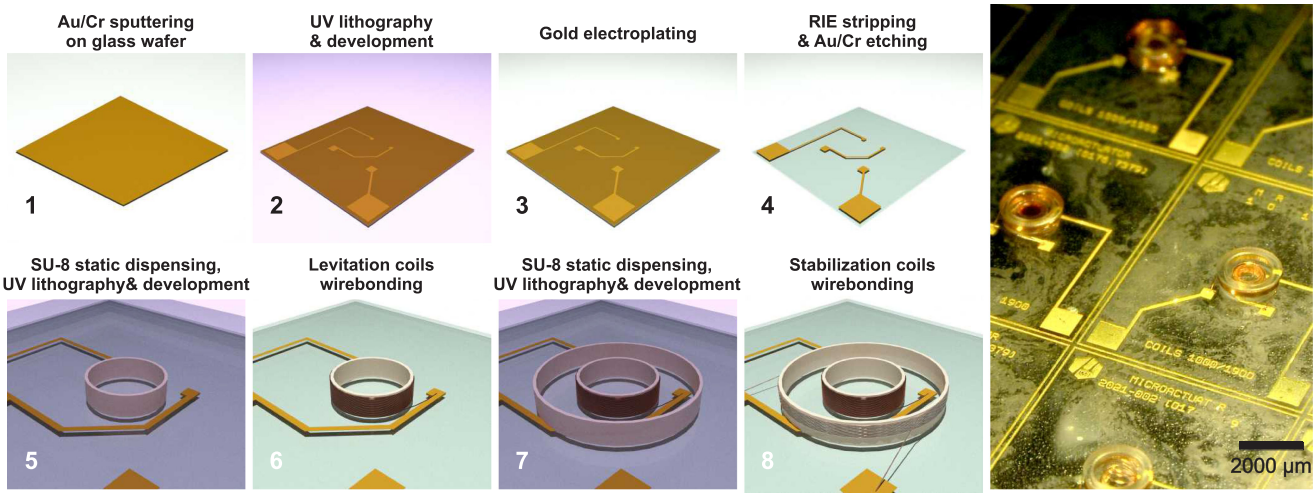

Fig. 1. (a) Schematic representation of the fabrication steps. (b) Fabricated array of nested two 3-D microcoil structures.

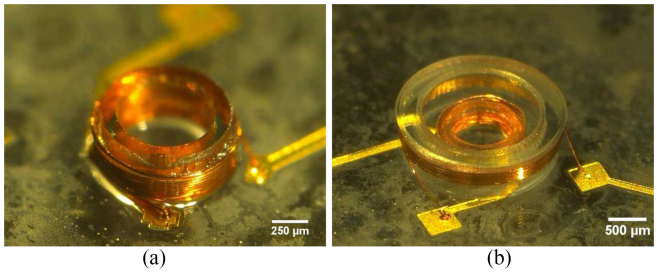

Fig. 2. Fabricated inner coil and nested two-coil structure. (a) Inner coil having a diameter of 1000 µm and 14 number of windings. (b) Outer coil having a 1900 µm and eight number of windings.

application as 3D-ILMS. In particular, the fabricated 3D-ILMS was able, for the first time, to levitate the reduced size of a disc-shaped proof mass of a diameter of 1100 µm at a height up to 45 µm.

II. MICROFABRICATION

Fig. 1(a) depicts the established multiple-step microfabrication process for the nested microcoils. *Steps 1 to 4* illustrate the fabrication of electrode array following the standard procedure previously developed for the solenoid microcoils [Kratt 2010, Lu 2014a, 2014b, Beyaz 2018]. While the gap between posts in the fabricated coil structure is only 250 µm and constrains the access to the electric pads of the wire-bonder with installed the smallest commercially available bottleneck capillary of 600 µm diameter. In order to overcome this issue, the following fabrication *Steps 5 to 8* were developed.

Briefly, in *Step 1*, Mempax glass wafer of 100 mm diameter and 525 µm thickness (supplied by Schott GmbH) was sputtered with a chromium of 20 nm as adhesion promoter and a gold of 60 nm. In *Step 2*, SU-8 3025 negative photoresist (supplied by Kayaku Advanced Materials, Inc.) was spin-coated to achieve 20 µm thickness, soft-baked at 95 °C for 15 min, exposed with 365 nm ultraviolet (UV) radiation (EVG 620, Thailner GmbH) of 360 mJ cm $^{-2}$ dose, postexposure baked for 4 min and developed in poly(ethylene glycol) methyl ether acrylate (PEGMEA, supplied by Spec EM Switzerland GmbH) and isopropyl alcohol (IPA, supplied by VWR). After development in *Step 3*, the open structures were electroplated with gold at 0.2 mA dm^{-1} for 40 min to achieve $\sim$ 5 µm of electrode pads height. In *Step 4*, the remaining SU-8 stripped with the freon (CF_4) plasma etching at 1200 W for 40 min (STP2020, R3T) followed by the chemical etching of gold and chromium.

Step 5 shows the microfabrication starting from the inner post. The posts were microfabricated with viscous SU-8 2150 (supplied by Kayaku Advanced Materials, Inc.), which allows the preparation of the structures with a high aspect ratio [Gaudet 2006]. SU-8 2150 was statically dispensed through a syringe of $\sim$ 5 mL volume on the wafer placed on the balanced hot plate at 75 °C. After dispensing, the hot plate was ramped to 95 °C at 0.15 °C/min and soft-baked for 9 h, and cooled to room temperature for six hours. This volume allowed the preparation of $\sim$ 500 µm thick posts. The lithography was performed with a dose of 2000 mJ·cm $^{-2}$, following the saturation dose for thick SU-8 structures [Gaudet 2006]. A specific postexposure backing cycle was applied to achieve the best adhesion of the posts. The microstructures were developed in PEGMEA with ultrasonic bath (Sonorex Super 10P, BANDELIN electronic GmbH) for 40 min and then kept in IPA for 10 min, and the procedure was repeated. The provided dose promoted better adhesion to the glass substrate but caused overexposure of the posts, resulting in an increase of the post width about 50 µm, and some residual SU-8 remained adhered to the electrode pads. Therefore, the additional plasma stripping with freon was employed for 20 min to remove this residual SU-8 and reduce the posts wall sizes. In *Step 6*, the coil winding was performed on ESEC 3100 CU Wirebonder using 25 µm insulated copper wire (X-Wire) provided from Microbonds. The complications due to the selection of the coated wire were taken into consideration, and the bond parameters were chosen appropriately to ensure a stable and repeatable process, such as temperature, ultrasonic energy, force, and bonding time [Kratt 2010]. The coils were wound around the inner posts using the custom-made trajectory implemented in the native wire-bonder program. In *Steps 7 and 8*, the microfabrication was repeated for the outer posts, and solenoid coils were wound on them in the opposite

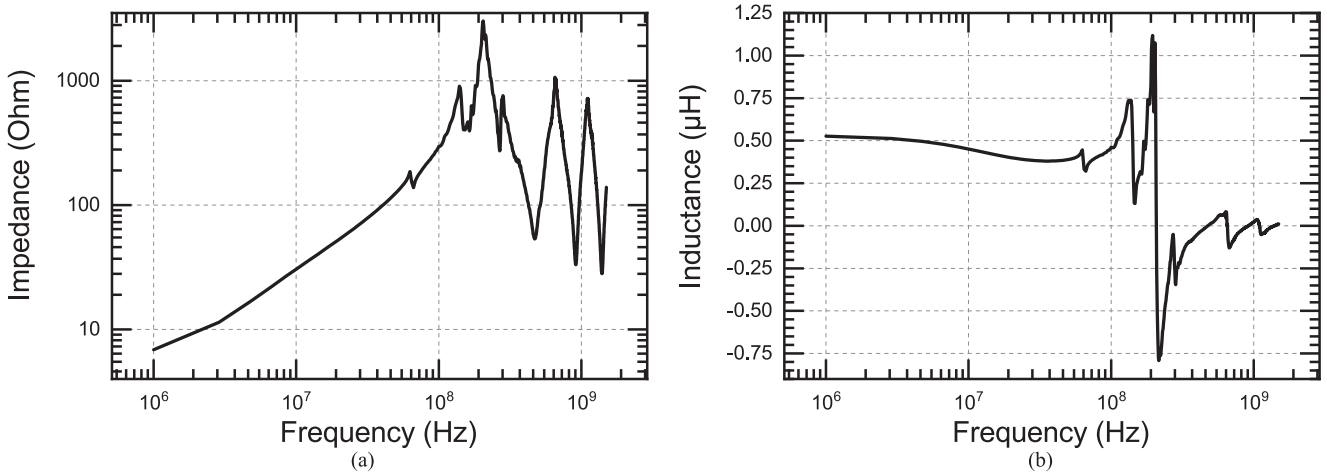

Fig. 3. (a) Impedance and (b) inductance of the nested microcoil. The resonance frequency determined at 207 MHz.

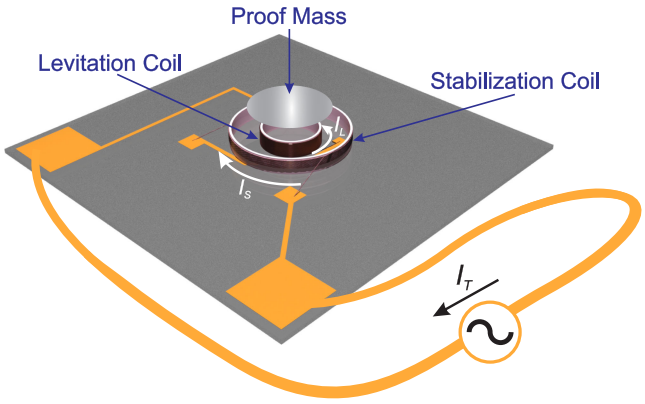

Fig. 4. Schematic of 3D-ILMA with levitated proof mass: I_L is an electric current in the levitation coil, I_S is an electric current in the stabilization coil, and I_T is a total electric current from the power supply.

direction to keep the current in antiphase. The number of windings was reduced from standard due to the implementation of plasma etching, which affected the designed performance of the microcoil. Fig. 1(b) shows a fabricated array of nested microcoils prior to dicing. The single chips were diced with the UV laser system Acsys Piranha II operating at 355 nm wavelength with 10 ns pulse duration and 20 kHz repetition rate.

Fig. 2 shows a successfully implemented fabrication procedure with a complete nested microcoil. The typical hollow levitation post shown in Fig. 2(a), which has a diameter of 1000 μm, wound around the post for 14 windings with ∼30 μm pitch, matching with the post height, resulted to ∼400 μm after freon plasma treatments. Fig. 2(b) depicts the complete device with a finalized outer post of 1900 μm diameter and eight windings for the stabilization microcoil, where the first revolution was initialized at 200 μm to match with the final loop of inner microcoil.

III. MEASUREMENTS

The nested microcoils were tested with a radio frequency impedance analyzer (Agilent E4991 A) to estimate the impedance and the inductance in a range between 1.5×10^3 MHz. Fig. 3 depicts the impedance and the inductance with the coupled levitation and stabilization coils.

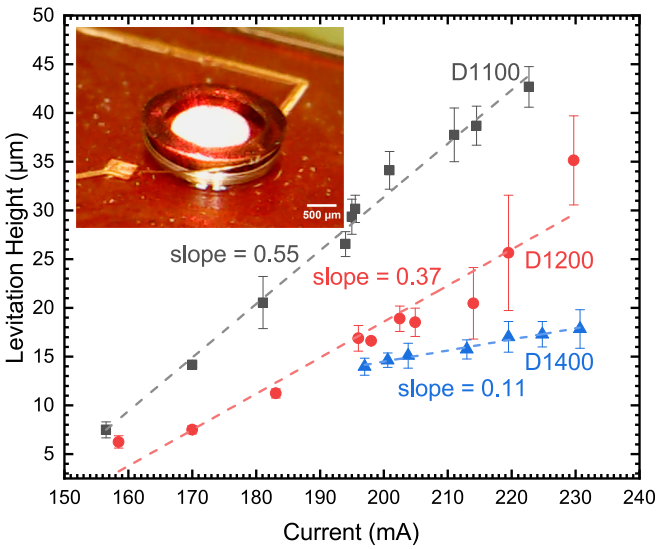

Fig. 5. Levitation height against the applied coil electric current. In the inset, a successful levitation of the 1200 μm diameter proof mass is shown.

The microcoil electrical parameters from the impedance spectroscopy were picked at the operation frequency of 10 MHz, and showed an impedance of 31.44 Ω, a resistance of 11.70 Ω, and the inductance of 4.48×10^{-7} H. The resonant frequency increased to 207 MHz from 111 MHz in comparison to the previous design [Lu 2014b]. Using Wheeler's formula, theoretical inductance L was calculated only for the levitation coil at 2.3×10^{-7} H, which drops in one order comparatively to the larger size design with 1.1×10^{-6} H [Lu 2014b]. Using the microcoil inductance, the generated magnetic field B can be calculated through relation(1)

$$B = \frac{LI}{NA} = \frac{5\pi\mu_0 NI}{9r + 10h_{\text{coil}}} \tag{1}$$

where I is the supplied current, N is the number of windings, A is the area, $\mu_0 = 4\pi 10 \times 10^{-7}$ H m^1 is the free space permeability, r is the radius of the coil and h_{coil} is the microcoil height. However, the maximal generated magnetic field at applied current of 150 mA

for the levitation coil is estimated at 1.55 mT for the fabricated 3D-ILMS against 1.26 mT for the larger size microstructure as reported in Lu [2014b]. Thus, the size reduction of coils increases the generated magnetic field.

Fig. 4 depicts a schematic of the experimental setup, where the levitation of an electrically conductive proof mass is achieved by excitation of the nested 3-D inductive microcoil with an ac current. This excitation induces eddy currents in the proof mass, and the interaction between the magnetic field generated by these eddy currents and the coil excitation current gives rise to the levitation force. A stabilization coil outside of the levitation coil prevents the proof mass from sliding off when the current is applied, which provides lateral stability [Shearwood 1996; Poletkin 2021].

To demonstrate the application of the fabricated coil structure as 3D-ILMS, proof masses were machined from Al film of 25 μm in a disk shape of 1100, 1200, and 1400 μm diameter using the previously mentioned UV laser system and having the mass of 60, 75, and 100 ng, respectively. Then, the nested microstructure was connected to the in-house built current amplifier with H-bridge configuration [Vlnieska 2020], controlling the current supply from the power source (Velleman LABPS3010SM) at the 10 MHz operation frequency. A levitation height of proof mass was tested with a laser sensor (Panasonic HL-G103-S-J) and measured from the top surface of the inner post.

Fig. 5 shows the levitation heights for three PMs having aforementioned diameters against the ac current measured in root mean square values. The stable levitation was observed for the PM of a 1100 μm diameter at the smallest height of 7.5 μm and 156 mA coil current. The highest current was not supplied above 230 mA, due to excess heating in 3D-ILMS and followed by its burning. All tested proof mass sizes follow the linear functions with the slopes depicted in the graph.

Inset of Fig. 5 shows a micrograph with the successful levitation of the proof mass of 1400 μm diameter and reflection of the laser beam from the aluminum film. In some cases, the positioning of stabilization coils lays out from the center of the inner coils and has some height difference between both sets of posts. Therefore, these issues promoted the shift of the proof mass to the levitation coil central position.

IV. CONCLUSION

We have developed the technological approach that, allowed us to fabricate the nested coil structure for 3D-ILMS with a smaller diameter of 1900 μm in comparison to previously reported 3D-ILMS structures having a 3800 μm diameter. The measurements showed that the miniaturized microcoil structure improved electromagnetic performance compared to previous 3D-ILMS designs. In particular, the microcoils inductance reduced to 4.48×10^{-7} H, which enabled a twofold increase in the self-resonance frequency to 207 MHz. The structure is able to generate higher magnetic field of 1.55 mT against 1.26 mT. Also, we demonstrated the successful levitation of the 1100 μm diameter disc-shaped PM, which is the smallest one among all previously reported 3D-ILMSs [Lu 2014a]. This study shows great potential in the further size reduction for a solenoid nested microcoil structure, up to 200 μm [Kratt 2010], in order to further improve the device efficiency for applications where the homogenous concentrated magnetic field is needed.

ACKNOWLEDGMENT

The work of Emil R. Mamleyev, Jan G. Korvink, and Kirill Poletkin was supported by the Deutsche Forschungsgemeinschaft (DFG, German Research Foundation) SPP 2206 Priority Program under Grant KO 1883/26-1. Emil R. Mamleyev thanks A. N. Julius for her help with the proof mass preparation, Dr. O. Nassar for his help with the impedance spectroscopy and conducted measurements, H. Fornasier, M. Zakharova, Dr. U. Köhler, and all cleanroom staff for their great cooperation, expertise, and advice on technological issues during microfabrication.

REFERENCES

Beyaz M I, Baelhadj H C, Habibiabad S, Adhikari S S, Davoodi H, Badilita V (2018), "A non-resonant kinetic energy harvester for bioimplantable applications," *Micromachines*, vol. 9, 217, doi: 10.3390/mi9050217.

Gaudet M, Camart J-C, Buchaillot L, Arscott S (2006), "Variation of absorption coefficient and determination of critical dose of SU-8 at 365 nm," *Appl. Phys. Lett.*, vol. 88, 024107, doi: 10.1063/1.2164390.

Kratt K, Badilita V, Burger T, Korvink J G, Wallrabe U (2010), "A fully MEMS-compatible process for 3D high aspect ratio micro coils obtained with an automatic wire bonder," *J. Micromechanics Microeng.*, vol. 20, 015021, doi: 10.1088/0960-1317/20/1/015021.

Lu Z, Poletkin K, den Hartogh B, Wallrabe U, Badilita V (2014a), "3D micro-machined inductive contactless suspension: Testing and modeling," *Sensors Actuators A: Phys.*, vol. 220, pp. 134–143, doi: 10.1016/j.sna.2014.09.017.

Lu Z, Poletkin K, Wallrabe U, Badilita V (2014b), "Performance characterization of micromachined inductive suspensions based on 3D wire-bonded microcoils," *Micromachines*, vol. 5, pp. 1469–1484, doi: 10.3390/mi5041469.

Poletkin K (2020), *Levitation Micro-Systems: Applications to Sensors and Actuators*. Berlin, Germany: Springer Nature, doi: 10.1007/978-3-030-58908-0.

Poletkin K (2021), "On the static pull-in of tilting actuation in electromagnetically levitating hybrid micro-actuator: Theory and experiment," *Actuators*, vol. 10, 256, doi: 10.3390/act10100256.

Poletkin K V, Lu Z, Moazenzadeh A, Mariappan S G, Korvink J G, Wallrabe U, Badilita V (2016), "Polymer magnetic composite core boosts performance of three-dimensional micromachined inductive contactless suspension," *IEEE Magn. Lett.*, vol. 7, 1307603, doi: 10.1109/LMAG.2016.2612181.

Poletkin K V, Asadollahbaik A, Kampmann R, Korvink J G (2018), "Levitating micro-actuators: A review," *Actuators*, vol. 7, 17, doi: 10.3390/act7010001.

Shearwood C (1996), "Electro-magnetically levitated micro-discs," in *Proc. IEE Colloq. Microeng. Appl. Optoelectronics*, pp. 6/1–6/3, doi: 10.1049/ic:19960241.

Shearwood C, Ho K, Williams C, Gong H (2000), "Development of a levitated micromotor for application as a gyroscope," *Sensors Actuators A: Phys.*, vol. 83, pp. 85–92, doi: 10.1016/S0924-4247(00)00302-2.

Simon M, Heflinger L, Geim A (2001), "Diamagnetically stabilized magnet levitation," *Amer. J. Phys.*, vol. 69, pp. 702–713, doi: 10.1119/1.1375157.

Vlnieska V, Voigt A, Wadhwa S, Korvink J, Kohl M, Poletkin K (2020), "Development of control circuit for inductive levitation micro-actuators," *Proceedings*, vol. 64, 39, doi: 10.3390/IeCAT2020-08479.